Chemistry & Biology, Vol. 12, 1137–1143, October, 2005, ©2005 Elsevier Ltd All rights reserved. DOI 10.1016/j.chembiol.2005.08.016

Genes Encoding Enzymes Responsible for Biosynthesis of L-Lyxose and Attachment of Eurekanate during Avilamycin Biosynthesis

Carsten Hofmann,[1,3] Raija Boll,[1,3] Björn Heitmann,[2] Gerd Hauser,[2] Clemens Dürr,[1] Anke Frerich,[1] Gabriele Weitnauer,[1] Steffen J. Glaser,[2,*] and Andreas Bechthold[1,*]

[1]Institut für Pharmazeutische Wissenschaften
Pharmazeutische Biologie und Biotechnologie
Albert-Ludwigs-Universität Freiburg
Stefan-Meier-Strasse 19
79104 Freiburg
Germany

[2]Institut für Organische Chemie und Biochemie
Technische Universität München
Lichtenbergstraße 4
85747 Garching
Germany

Summary

The oligosaccharide antibiotic avilamycin A is composed of a polyketide-derived dichloroisoeverninic acid moiety attached to a heptasaccharide chain consisting of six hexoses and one unusual pentose moiety. We describe the generation of mutant strains of the avilamycin producer defective in different sugar biosynthetic genes. Inactivation of two genes (*aviD* and *aviE2*) resulted in the breakdown of the avilamycin biosynthesis. In contrast, avilamycin production was not influenced in an *aviP* mutant. Inactivation of *aviGT4* resulted in a mutant that accumulated a novel avilamycin derivative lacking the terminal eurekanate residue. Finally, AviE2 was expressed in *Escherichia coli* and the gene product was characterized biochemically. AviE2 was shown to convert UDP-D-glucuronic acid to UDP-D-xylose, indicating that the pentose residue of avilamycin A is derived from D-glucose and not from D-ribose. Here we report a UDP-D-glucuronic acid decarboxylase in actinomycetes.

Introduction

Avilamycins are oligosaccharide antibiotics isolated from *Streptomyces viridochromogenes* Tü57 (*S. viridochromogenes* Tü57) [1] (Figure 1). Avilamycin A, the main compound produced by the strain was shown to be active against many Gram-positive bacteria, including emerging problem organisms such as vancomycin-resistant enterococci, methicillin-resistant staphylococci, and penicillin-resistant pneumococci [2]. Evernimicin (Ziracin), which is structurally very similar to avilamycin, was under investigation for approval by Schering-Plough. Due to side effects and its poor water solubility, further development was stopped in 2000 [3]. Evernimicin and avilamycin were shown to inhibit protein biosynthesis by binding to the 50S ribosomal subunit of the bacterial ribosomes [4–6]. It was suggested that they interact with the ribosomal A-site and interfere with initiation factor IF2 and tRNA binding.

Recently, we reported the sequence of the complete biosynthetic gene cluster for avilamycin A [7]. Based on sequence similarities of the deduced proteins to enzymes of known functions, putative biosynthetic pathways to each sugar were proposed. Gene disruption experiments with putative methyltransferase genes [2] have led to new avilamycins with enhanced water solubility (named gavibamycins) (Figure 1) and after deletion of *aviB1* and *aviO2* an avilamycin derivative (gavibamycin O) was obtained lacking the acetyl residue at position C-4 of the eurekanate moiety of avilamycin A [8].

It is most likely that the biosynthesis of avilamycin A starts with the formation of the unusual disaccharide consisting of the pentose L-lyxose and the hexose D-mannose. The attachment of the progenitor of eurekanate to the C-4 position is a further plausible step toward the formation of the heptasaccharide side chain. However, insights regarding early steps in the biosynthesis of avilamycin A are sparse.

Our recent elucidation of the avilamycin gene locus revealed several deoxy sugar biosynthetic genes and four glycosyltransferase genes. Based on sequence homologies AviD, a putative dNDP-glucose synthetase, was discussed to be the entrance enzyme of the D-olivose and 2-deoxy-D-evalose pathway. AviP, a putative phosphatase, was thought to be the first enzyme of the pathway leading to L-lyxose and AviE2, a putative 4,6-dehydratase, leading to eurekanate.

In order to gain insights into the biosynthesis of the avilamycin molecule, we now report classical feeding experiments, the generation of four mutants of the avilamycin producer with deletion in different sugar biosynthetic and glycosyltransferase genes and the overexpression of *aviE2* in *E. coli*.

Our results indicate that L-lyxose derives from D-glucose by decarboxylation and that AviGT4 is a glycosyltransferase involved in the formation of the orthoester linkage between L-lyxose and the eurekanate residue.

Results and Discussion

Feeding of Labeled D-Glucose

Labeled glucose (U-^{13}C glucose, 1-^{13}C glucose) was added to the culture medium inoculated with *S. viridochromogenes* Tü57. Avilamycin A was isolated by reverse phase chromatography and preparative high pressure liquid chromatography-mass spectrometry (HPLC-MS). In the nuclear magnetic resonance (NMR) spectra of the labeled compound obtained by feeding 1-^{13}C glucose (Figure 2a), the signal volumes of all carbons in the C-1 positions are identical (within error limits of 11%) and ~8-fold larger than the signal volumes of carbons at other positions. This increased occurrence of ^{13}C at the C-1 positions indicates usage of D-glucose as a precursor for all components, which was in contrast to the assumption that ribose-5-phosphate is the precursor of L-lyxose [7].

*Correspondence: glaser@ch.tum.de (S.J.G.), andreas.bechthold@pharmazie.uni-freiburg.de (A.B.)

[3]These authors contributed equally to this work.

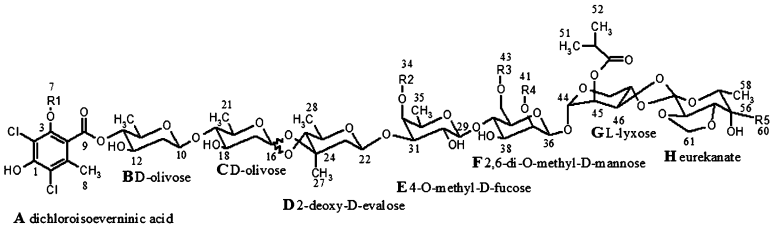

Figure 1. Structure of Avilamycin and Gavibamycin Derivatives

Strain	Substance	R1	R2	R3	R4	R5
S. viridochromogenes Tü57	Avilamycin A	CH_3	CH_3	CH_3	CH_3	$COCH_3$
S. viridochromogenes Tü57	Avilamycin C	CH_3	CH_3	CH_3	CH_3	$CH(OH)CH_3$
S.viridochromogenes GW4	Gavibamycin A1	H	CH_3	CH_3	CH_3	$COCH_3$
S.viridochromogenes GW4	Gavibamycin A3	H	CH_3	CH_3	CH_3	$CH(OH)CH_3$
S.viridochromogenes GW4-GW2	Gavibamycin C1	H	CH_3	H	CH_3	$COCH_3$
S.viridochromogenes GW4-GW5	Gavibamycin E1	H	H	CH_3	CH_3	$COCH_3$
S.viridochromogenes GW4-GW6	Gavibamycin I1	H	CH_3	CH_3	H	$COCH_3$
S.viridochromogenes GW2	Gavibamycin J1	CH_3	CH_3	H	CH_3	$COCH_3$
S.viridochromogenes GW5	Gavibamycin K1	CH_3	H	CH_3	CH_3	$COCH_3$
S.viridochromogenes GW6	Gavibamycin L1	CH_3	CH_3	CH_3	H	$COCH_3$
S.viridochromogenes ITO2	Gavibamycin O	CH_3	CH_3	CH_3	CH_3	H

The NMR analysis of the U-^{13}C glucose feeding experiment (Figure 2b) allowed to identify D-glucose as the source of the methyl group at position C-5 of the eurekanate residue. The signal of 35 (see Figure 1 for nomenclature) is representative for a methyl group derived directly from D-glucose, whereas position 27 is an example for a CH_3-group attached to the sugar ring at a later stage of the biosynthesis. (This has been shown by ^{13}C-labeled L-methionine feeding experiments described in [7].) Integration of a variety of signals (among them the ones of positions 35 and 58) showed that the average degree of ^{13}C-labeling was ~20%, whereas position 27 was labeled to only ~8%, indicating that position 58 is derived directly from D-glucose. The shapes of the signals prove this assumption. The signals of 35 and 58 show small, uncoupled singlets and large doublets caused by the $^1J_{13C,13C}$ couplings to the adjacent carbons in the sugar rings (positions 33 and 57, respectively). Thus, a labeled methyl group has a very high probability (>90%) of being connected to a ^{13}C-atom. Because of the average degree of ^{13}C-labeling (~20%), this is possible only if the complete C_6 scaffold of the U-^{13}C glucose, including the methyl group, is inserted as a whole during biosynthesis. On the other hand, the signal of position 27 shows a large singlet and a small doublet. For this position, therefore, the probability of being connected to a ^{13}C in the ring (at position 24) is in the range of the average degree of labeling, confirming the subsequent addition of the methyl group to the U-^{13}C glucose scaffold.

Because evernimicin, another orthosomycin antibiotic, lacks a methyl group at position C-5 of eurekanate, different biosynthetic pathways to both antibiotics have to be discussed.

Generation of *S. viridochromogenes* Tü57Δ*aviD*, *S. viridochromogenes* GW4Δ*aviP*, *S. viridochromogenes* GW4Δ*aviE2*, and *S. viridochromogenes* GW4Δ*aviGT4*

For generation of mutants, gene inactivation experiments were carried out. As hosts we used *S. viridochromogenes* Tü57 and *S. viridochromogenes* GW4, a mutant lacking the methyltransferase gene *aviG4* [7]. Plasmids were constructed as described in Experimental Procedures, allowing the replacement of the wild-type gene by a mutated allele in *S. viridochromogenes* Tü57. The deletions within the genes were confirmed by polymerase chain reaction (PCR) (*aviD*, *aviP*, *aviE2*, *aviGT4*) and by Southern hybridization (*aviD*, *aviP*, *aviE2*). PCR fragments obtained from double crossover mutants (*S. viridochromogenes* Tü57Δ*aviD*, *S. viridochromogenes* GW4Δ*aviP*, *S. viridochromogenes* GW4Δ*aviE2*,

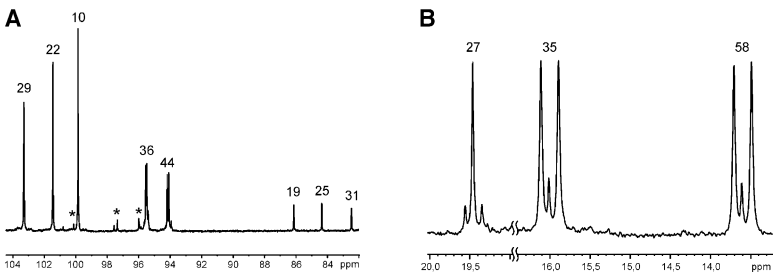

Figure 2. Sections of the ^{13}C-1D-NMR Spectrum

(A) Section of the ^{13}C-1D-NMR spectrum (^{1}H-decoupled) of avilamycin after the feeding experiment with 1-^{13}C glucose showing the signals of five partially labeled (10, 22, 29, 36, and 44) and three unlabeled (19, 25, and 31) carbons. The numbering of the resonances corresponds to Figure 1. Signals marked with asterisks are impurities. The chemical shifts for carbons 36 and 44 show slight variations for avilamycin A, avilamycin B and avilamycin C which were abundant at a ratio of approximately. 40:10:50 (determined by HPLC and NMR).

(B) Two sections of the ^{13}C-1D-NMR spectrum (^{1}H-decoupled) of the U-^{13}C glucose feeding experiment comparing the signal of position 58 with the ones of 27 and 35 (see Figure 1 for nomenclature). The signal of 35 is representative for a methyl group derived directly from D-glucose whereas position 27 is an example for a CH_3-group attached to the sugar ring at a later stage of the biosynthesis [7].

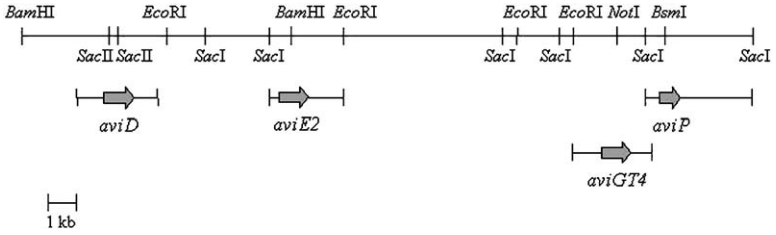

Figure 3. Region of the Avilamycin Biosynthetic Gene Cluster Containing *aviD*, *aviE2*, *aviGT4*, and *aviP*

Only genes investigated during this study are shown as arrows. Fragments containing each individual gene used for the generation of inactivation constructs as well as important restriction sites are indicated.

and *S. viridochromogenes GW4ΔaviGT4*) using primers aviD-F2/aviD-R2, aviP-A/aviP-B, aviE2P-F/aviE2P-R, and aviGT4-F2/aviGT4-R2, respectively, could not be digested by SmaI, NotI, BamHI, and NotI, respectively (Figure 3), whereas the PCR fragments obtained from *S. viridochromogenes* Tü57 and *S. viridochromogenes* GW4 could be digested by the enzymes. To determine clearly that the mutation event affected only the desired genes and not other genes, *aviE2* and *aviGT4* were ligated behind the *ermE** promoter of pSET-1cerm and were introduced by protoplast transformation into the corresponding mutants. Complementation of *S. viridochromogenes* Tü57Δ*aviD* was achieved by expression of a 5 kb fragment containing *aviD* behind the native promoter. Avilamycin (gavibamycin) production was restored in each case.

Isolation and Identification of Avilamycin Derivatives

S. viridochromogenes Tü57, *S. viridochromogenes* GW4, *S. viridochromogenes* Tü57Δ*aviD, S. viridochromogenes* GW4Δ*aviP, S. viridochromogenes* GW4Δ*aviE2* and *S. viridochromogenes* GW4Δ*aviGT4* were grown under the conditions described in Experimental Procedures. Extracts were analyzed by thin-layer chromatography (TLC), HPLC-UV/Vis, and HPLC-ESI (electrospray ionization)-MS. Avilamycin A and C were detected in *S. viridochromogenes* Tü57 (wild-type strain), gavibamycins A1 and A3 were detected in *S. viridochromogenes* GW4 and *S. viridochromogenes* GW4Δ*aviP*. No avilamycin derivative could be observed in *S. viridochromogenes* Tü57Δ*aviD* and in *S. viridochromogenes* GW4Δ*aviE2*. The HPLC-ESI-MS analysis of the mutant *S. viridochromogenes* GW4Δ*aviGT4* revealed that none of the gavibamycins typically found in *S. viridochromogenes* GW4 were produced. Instead, a novel compound with the typical UV/Vis spectrum of the gavibamycin chromophore was identified. Its molecular ion with *m/z* 1189 $[M-H]^-$ displayed the diagnostic isotope pattern distinctive for the double-chlorinated gavibamycins (Figure 4). Hence, the compound was very likely a gavibamycin derivative, referred to as gavibamycin P1. The mass difference of 198 amu compared to gavibamycin A1 (*m/z* 1387 $[M-H]^-$) produced by *S. viridochromogenes* GW4 indicated a lacking eurekanate moiety, the terminal residue of the oligosaccharide chain (Figure 4). To corroborate this structure, a comparative fragmentation analysis with an atmospheric pressure chemical ionization (APCI) source was carried out with gavibamycin A1 serving as reference. For this purpose, gavibamycins P1 and A1 were purified from *S. viridochromogenes* GW4Δ*aviGT4* and *S. viridochromogenes* GW4, respectively. Subsequent fragmentation analysis revealed an analogous fragmentation pattern for both compounds in the negative ionization mode (Figure 4). Two groups of fragments could be observed. First, fragments with the isotope profile of the chlorinated orsellinic acid and equal mass between gavibamycin P1

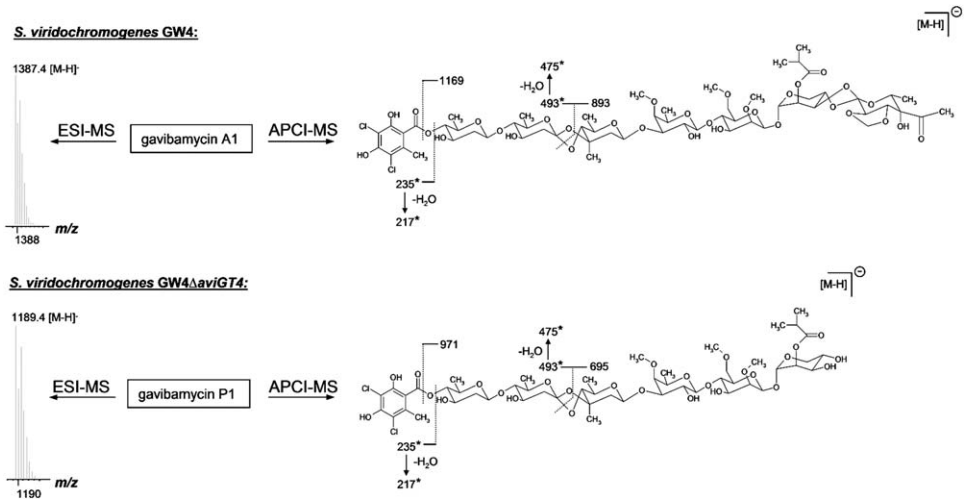

Figure 4. Mass Spectrometry of Gavibamycin A1 and P1

ESI-MS analysis yields the deprotonated molecule with *m/z* 1387 and *m/z* 1189, respectively. In both cases, the diagnostic isotope pattern reflects the presence of the double-chlorinated orsellinic acid. APCI-MS analysis yields an analogous fragmentation pattern of both compounds. The fragments labeled with an asterisk display the isotope pattern of the orsellinic acid. All further fragments differ in 198 amu between gavibamycin A1 and P1, representing the lacking terminal eurekanate residue in gavibamycin P1.

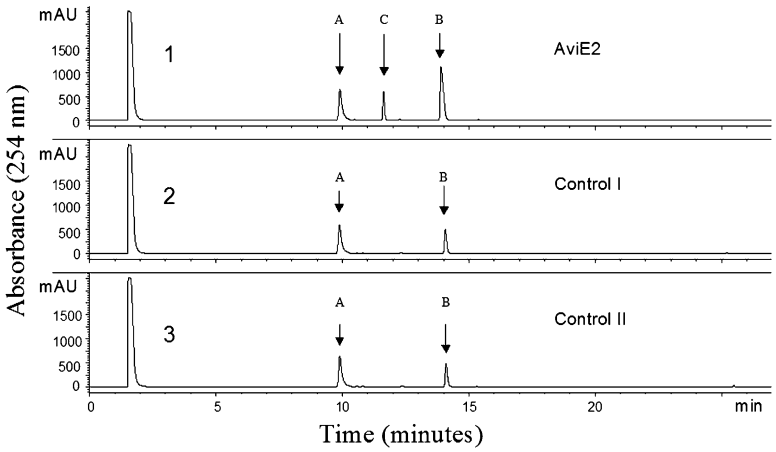

Figure 5. In Vitro Conversion of UDP-D-GlcA Acid to UDP-D-Xylose by AviE2

The results of different incubations analyzed by HPLC are shown as follows: (1) Incubation containing AviE2; (2) incubation containing enzyme eluted from a Ni-NTA column obtained from *E. coli* cultures containing pRSETB (vector without insert); (3) no enzyme. Chromatographic peaks corresponding to NAD^+ (A), UDP-GlcA (B), and UDP-D-xylose (C) are indicated by arrows.

and A1. Second, fragments that differed in 198 amu from those derived from gavibamycin P1 displaying the lower mass. These fragments represent a terminally shortened oligosaccharide chain and therefore can plausibly explain the structure of a gavibamycin lacking the eurekanate residue (Figure 4).

Although it was expected that the *aviD* mutant would not produce any avilamycin derivative, production of avilamycins by the *aviP* mutant and nonproduction by the *aviE2* mutant were surprising results. We concluded that AviP is not involved in the formation of the L-lyxose moiety and that AviE2 is not an NDP-glucose 4,6-dehydratase involved in the eurekanate biosynthesis.

AviGT4 Is Involved in the Formation of the Linkage between L-Lyxose and Eurekanate

Because our data show that the derivative gavibamycin P1 produced by *S. viridochromogenes* GW4Δ*aviGT4* lacks the terminal eurekanate moiety and because AviGT4 matches GTs that are involved in cell envelope and lipopolysaccharide biosynthesis, we conclude that AviGT4 is essential for the transfer of the eurekanate residue to the L-lyxose moiety. For now, we cannot predict whether AviGT4 is responsible for the formation of a "simple" glycosidic bond or whether it catalyzes the entire formation of the orthoester. Results of the *aviGT4* inactivation experiments revealed that the disaccharide L-lyxose-eurekanate is not the starter molecule for avilamycin A biosynthesis. It now seems likely that the avilamycin biosynthesis begins within the formation of the 1→1 linked disaccharide D-mannopyranosyl-L-lyxose instead.

AviE2, a Decarboxylase as Key Enzyme for the Generation of L-Lyxose during Avilamycin A Biosynthesis

Results of the knockout experiments prompted us to perform a careful BLAST analysis of the encoded AviE2. AviE2 is homologous to other enzymes that oxidize the C-4 position of certain UDP-sugars, such as UDP-galactose epimerase [9], dTDP-glucose-4,6-dehydratase [10], and eukaryotic UDP-glucuronic acid (UDP-GlcA) decarboxylases [11, 12], all belonging to the short chain dehydrogenase/reductase superfamily [13, 14]. This group of proteins is characterized by high structural similarity and the presence of specific sequence motifs despite low overall sequence identity [15]. AviE2 retains the glycine-rich NAD^+ binding motif GXXGXXG represented by amino acids $G_{15}GAG_{18}FIG_{21}$. A conserved acidic amino acid (D_{49} in AviE2) is also present. This acidic amino acid interacts with adenine ribose hydroxyl groups and is present in all NAD^+ and FAD^+ binding members of the SDR family [14]. The sequence YXXXK, together with a conserved T/S residue, is responsible for the NAD^+ dependent oxidation of a sugar hydroxyl group at position C-4 in UDP-sugars, and these motifs are also present in AviE2, represented by residues T_{134} and $Y_{163}DEAK_{167}$. Serine and lysine are suggested to activate tyrosine to abstract the C-4 proton to yield a nucleotide-4-keto sugar intermediate [16]. A glutamate D_{164} (prevents ring flipping) and an arginine R_{318} (responsible for decarboxylation) are strictly conserved in UDP-GlcA decarboxylases [17]. Both are existing in AviE2. An aspartate, which is conserved in 4,6-dehydratases [18], is occupied by a serine (S_{135}) in AviE2. This serine has been shown to be involved in the decarboxylation process of UDP-decarboxylases [17]. To prove the function of AviE2, the corresponding gene was overexpressed in *E. coli* as His-tag fusion protein. Subsequent AviE2 characterization revealed this protein to be a UDP-GlcA-decarboxylase (Figure 5). The product of the AviE2 reaction was identified as UDP-D-xylose by HPLC-MS (Figure 6) and by NMR analysis. The chemical shifts measured in the 1D-spectra were in very good accordance with the literature [19] and, moreover, have been verified using the 2D-experiments described in Experimental Procedures. The $^3J_{H1,H2}$ coupling constant of 3–3.5 Hz (lit.: 3.5 Hz) confirmed the α-anomeric configuration of the UDP-pentose. The identification as UDP-D-xylose was based on the measured $^3J_{H3,H4}$ coupling constant of 9 ± 0.5 Hz (lit.: $^3J_{H3,H4}$(xylose) = 8.9 Hz; $^3J_{H3,H4}$(arabinose) = 3.4 Hz).

Replacement of the UDP-GlcA substrate with UDP-Glc or NAD^+ with $NADP^+$ yielded no product, indicating specificity of the reaction for UDP-GlcA and NAD^+. The activity obeyed Michaelis-Menten kinetics with a K_m of ~1.2 mM for UDP-GlcA, which is reasonable for this type of enzyme [14, 15]. The dexcarboxylation of UDP-D-GlcA to UDP-D-xylose is a common enzymatic step in the formation of pentoses for the primary metabolism [19, 20], but has never been described as enzymatic step in the formation of pentoses for the secondary metabolism in actinomycetes.

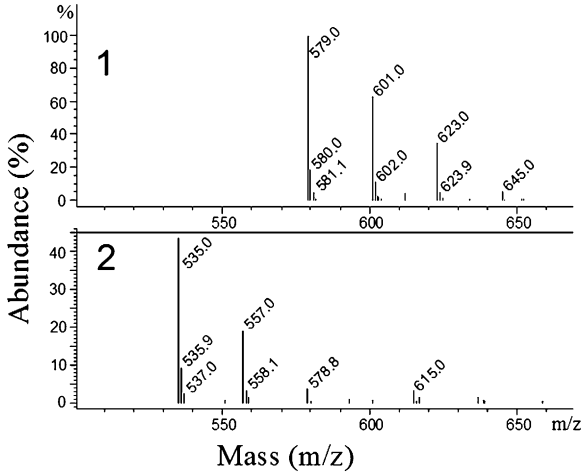

Figure 6. Electrospray Negative Ion Spectra of UDP-GlcA (1) and UDP-D-Xylose (2)

Besides the UDP-glucuronate peak ($[M-H]^-$ = 579.0), additional peaks appeared in the negative ion spectrum reflecting the presence of monosodiated ($[M + Na - 2H]^-$ = 601.0) and disodiated ($[M + 2Na - 3H]^-$ = 623.0) UDP-glucuronate. For UDP-D-xylose, peaks appeared at ($[M-H]^-$ = 535.0), ($[M + Na - 2H]^-$ = 557.0) and ($[M + 2Na - 3H]^-$ = 578.8.

The identification of AviE2 as a UDP-GlcA decarboxylase indicates that the formation of avilamycin A starts with the formation of UDP-L-lyxose from UDP-D-glucose. Thorson and coworkers proposed a similar biosynthetic pathway to the deoxypentose moieties of enediyne antitumor antibiotics. They found a UDP-glucose dehydrogenase encoding gene (*calS8*) in the calicheamicin gene cluster responsible for the conversion of UDP-D-glucose to UDP-D-GlcA and also a gene encoding a putative decarboxylating enzyme (CalS9) [21]. Interestingly, no UDP-glucose dehydrogenase encoding gene candidate has been detected in the avilamycin gene cluster so far. The conversion of UDP-D-xylose to UDP-L-lyxose requires two additional epimerization steps (Figure 7). There are candidates in the avilamycin gene cluster (*aviQ1*, *aviQ2*, *aviQ3*) that might be involved in these biosynthetic steps.

Significance

To our knowledge, this is the first report on avilamycin A biosynthetic enzymes involved in the formation of the hexasaccharide biosynthesis. Our data show that AviGT4 is involved in the formation of the unusual orthoester linkage between the eurekanate portion and L-lyxose. Gene inactivation as well as gene expression and biochemical experiments indicate that AviE2 is involved in the decarboxylation of UDP-GlcA to form UDP-D-xylose. Based on the increasing level of interest in new antibiotics, biosynthetic studies are of importance and will pave the way for the formation of novel derivatives in the future.

Experimental Procedures

Feeding Experiments

S. viridochromogenes Tü57 was grown on 1% malt extract, 0.4% yeast extract, and 0.4% glucose (pH adjusted to 7.5) [HA-medium] at 37ºC and 180 rpm. For avilamycin production, *S. viridochromogenes* Tü57 was grown at 28ºC in SG medium containing 2% glucose, 1% soy peptone, 0.1% $CaCO_3$, 20 mM L-valin, and 1 ml of 0.1% $CoCl_2$ (pH adjusted to 7.2). Then 100 mg/l of the U-^{13}C -glucose or 1-^{13}C -glucose was added after 24 and 48 hr. The avilamycins were isolated after 72 hr of cultivation and purified as described previously [2]. After purification, the substances were analyzed by ^{13}C-NMR.

Bacterial Strains, Plasmids, and Culture Conditions

DNA manipulation was carried out using *E. coli* XL-1 Blue MRF′ (Stratagene) as the host strain. Before transforming *S. viridochromogenes* strains, plasmids were propagated in *E. coli* ET 12567 (dam^-, dcm^-, hsdS, Cm^R) [22, 23] to obtain unmethylated DNA. *E. coli* strains were grown on Luria-Bertani (LB) agar or liquid medium containing the appropriate antibiotic. pBluescript SK^- ($pBSK^-$) and pBC-SK^- were from Stratagene; pUC19 was from New England Biolabs. Plasmid pSP1 [24], conferring erythromycin resistance, was a kind gift of Dr. S. Pelzer, and pSET152 [25], conferring apramycin resistance, was obtained from Eli Lilly & Co. The construction of pSET-1cerm has been described [26].

General Genetic Manipulation, PCR, and Sequence Analysis

Routine methods were performed as described [27]. Isolation of *E. coli* plasmid DNA, DNA restriction, DNA modification, and Southern hybridization were performed following the manufacturer's directions (Amersham Biosciences, Roche Diagnostics, Promega, Stratagene). *Streptomyces* protoplast formation, transformation, and protoplast regeneration were performed as described [28]. PCR was carried out using a GeneAmp PCR System 9700 (Applied Biosystems). Oligonucleotide primers from Qiagen are listed in the Supplemental Data. Computer-aided sequence analysis was done with the DNAsis software package (version 2.1, 1995; Hitachi Software Engineering). Database searches were performed with the BLAST 2.0 program [29] on the server of the National Center for Biotechnology Information, Bethesda, MD.

Construction of Gene Inactivation Plasmids

aviE2

AviE2, located on a 2.6 kb EcoRI/SacI fragment, was ligated into $pBCSK^-$ to generate plasmid pBC-aviE2. A unique BamHI restriction site was altered by BamHI restriction and subsequent treatment with T4 DNA polymerase and religation. DNA sequencing showed

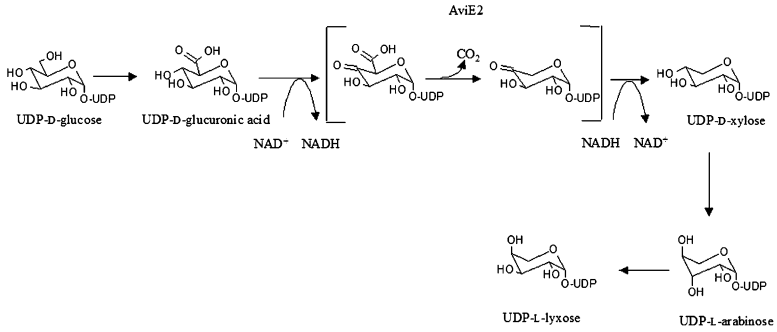

Figure 7. Hypothetical Biosynthetic Pathway from UDP-D-Glucose to UDP-L-Lyxose

that treatment with T4 DNA polymerase led to a 36 bp deletion in *aviE2*. After restriction with EcoRI and SacI, the insert was transferred to plasmid pSP1 to generate pSP-aviE2.

aviP

A 3.7 kb SacI fragment containing *aviP* was ligated in pBSK$^-$. A unique BsmI restriction site was used for modification by restriction with BsmI, treatment with T4 DNA polymerase and subsequent religation of the plasmid. DNA sequencing revealed the deletion of 25 bp in *avi*P.

After restriction with SacI and XbaI, the insert was ligated in plasmid pSP1. By restriction with NotI and following religation, the insert was shortened to 1.8 kb. The resulting construct was named pSP-aviP.

aviD

A 2.85 kb section including the entire reading frame of *aviD* was amplified by PCR. Primers aviD-F1 and aviD-R1, which introduced restriction sites for HindIII and BamHI, were used. This PCR fragment was cloned into pUC19 to give pUC19/aviD. By restriction with SacII and ligation of the remaining plasmid, a 291 bp fragment was deleted out of the gene *aviD.* The intended alteration was checked by DNA sequencing using the primer aviD-BS1. The altered 2.57 kb insert of pUC19/aviD-S was excised by HindIII and EcoRI and was ligated in the PstI and EcoRI sites of pSP1 after generation of blunt ends by the Klenow enzyme leading to the final inactivation plasmid pSP1/*aviD-S*.

aviGT4

A region of 2.8 kb containing *aviGT4* was amplified from chromosomal DNA using primers aviGT4-F1 and aviGT4-R1. The PCR product was ligated into the EcoRI and XbaI sites of pUC19. To shift the reading frame of *aviGT4*, the plasmid was linearized by digestion of a singular NotI site internal to *aviGT4* and treated with T4-polymerase to blunt the sticky ends. After religation, the intended alteration (correct fill-in) was confirmed by DNA sequencing. Finally, the EcoRI- XbaI- insert was cloned into pSP1, yielding pSP1_aviGT4i.

Construction of Complementation Plasmids for *aviE2*, *aviGT4*, and *aviD*

aviE2

For generation of the plasmid pSETerm-aviE2 used to complement the decarboxylase mutant, *aviE2* was amplified by PCR. As suitable restriction sites, EcoRI and XbaI were introduced upstream and downstream of the gene using oligonucleotide primers aviE2F and aviE2R. Plasmid pSET-1cerm was digested with MunI and XbaI to remove *urdGT1c*, and *aviE2* was cloned behind the *ermE** promoter after restriction of the PCR product using EcoRI and XbaI. The resulting complementation plasmid was named pSETerm-aviE2.

aviD

A 5 kb fragment including *aviD* was cut out of a 7.7 kb SacI fragment (P2S11) using BamHI and EcoRI. The fragment was cloned into the BamHI and EcoRI site of pSET152 to yield complementation construct pSET152/*aviD*.

aviGT4

A 2.8 kb fragment containing a*viGT4* was amplified from chromosomal DNA using primers aviGT4-F1 and aviGT4-R1. The PCR product was digested by EcoRI/XbaI and ligated into pSET-1cerm restricted by MunI/XbaI to yield pSETermE-aviGT4.

Expression and Purification of AviE2

The *aviE2* gene was PCR-amplified using NcoI-modified primer E2A and EcoRI-modified primer E2B and subcloned into the vector pRSETb (Invitrogen) to form plasmid pRSET-E2. DNA sequence of the coding region was confirmed by sequencing (4base lab).

For purification of expressed protein, *E. coli* strain BL21 (DE3) pLysS cells (Stratagene), carrying either pRSET-E2 with *aviE2* or the pRSETb vector alone, were grown in NZCYM medium containing 50 μg/ml carbenicillin and 30 μg/ml chloramphenicol to OD_{600}= 0.6. Protein expression was induced for 4 hr at 28ºC with 1mM isopropyl-β-D-thiogalactopyranoside. Cells were harvested by centrifugation and stored at −20ºC. The cell pellet from 100 ml culture was resuspended in 4 ml lysis buffer (NaH_2PO_4 50 mM, NaCl 300 mM, imidazol 10 mM) containing 1 mg/ml lysozyme and stored on ice for 30 min. After centrifugation, the supernatant fraction was used for purification.

Protein was bound to Ni-NTA agarose (Qiagen) and loaded on a column. The column was washed twice with washing buffer containing 20 mM imidazol. The protein was eluted with elution buffer containing 250 mM imidazol. SDS-PAGE of the starting material and the eluted fraction is shown in Figure 7.

Decarboxylase Assay

Standard analytical enzyme assays (200 μl) were performed at 23ºC for 60 min. One incubation mixture contained 40 mM Tris-HCl (pH 7,4), 1mM NAD^+, 1 mM UDP-GlcA and 1.3 mg/ml AviE2. Reactions were stopped by the addition of 200 μl of phenol-chloroform, vortex-mixed and subjected to centrifugation (14,000 rpm, 5 min, room temperature). The aqueous phase was reserved, and the organic phase was reextracted with 160 μl H_2O. The two aqueous phases were pooled and further purification was achieved by HPLC (Agilent 1100) on a 150 × 4.6 mm quaternary amine-silica gel ion exchange column (Zorbax 5 μm SAX, Agilent) run at 1.5 ml/min. After injection, the column was washed for 5 min with mobile phase A (5% glacial acetic acid in water) and then eluted with a 18 min linear gradient from 12% to 45% with solvent B (0.5 M NH_4HCO_3, pH 7 in water) and water. The LC eluent was split (Agilent splitter) 1:50 with water and transferred to a mass spectrometer (Agilent). The make-up pump was set to 0.5 ml/min. The mass spectrometer consisted of an electrospray chamber and a quadrupole detector. For NMR analysis, 12.9 mg UDP-GlcA was used in a 10 ml incubation mixture. After 8 hr, the product was purified by HPLC-MS, dissolved in water, relyophilized several times, exchanged twice with 99% D_2O, and then subjected to NMR analysis.

ESI- and APCI-MS Analysis

Mass spectrometry of purified gavibamycins A1 and P1 was performed on an Agilent 1100 series system optionally equipped with either an ESI or APCI chamber and a quadrupole detector. Samples were dissolved in 100% CH_3CN and directly applied to the ionization chamber with a 90:10 (CH_3CN:H_2O) eluent at a flow rate of 0.7 ml/min. To determine the $[M-H]^-$ molecular ions, ESI spectrometry was carried out using chamber settings as follows: drying gas flow, 12 l/min (nitrogen); drying gas temperature, 350ºC; nebulize pressure, 50 psig; capillary voltage (negative), 3kV. Samples were analyzed in the negative ionization mode with a mass range set to 400–1400 Da. For fragmentation analyses, APCI spectrometry was carried out under the following chamber conditions: drying gas flow, 12 l/min (nitrogen); drying gas temperature, 350ºC; nebulize pressure, 50 psig; vaporizer temperature, 450ºC; capillary voltage (negative), 3kV; corona current, 25 μA. Samples were analyzed in the negative ionization mode with a mass range set to 180–1450 Da.

NMR Analysis

The experiments were recorded in DMSO-d_6 at 295 K on Bruker DMX spectrometers (600 and 750 MHz) using 5 mm Shigemi tubes: ^{1}H-1D, ^{13}C-1D, COSY [30], TOCSY [31–33], ROESY [34] (mixing time: 150 ms), HSQC [35], HMBC [36], and HMQC-COSY [37]. All spectra were assigned using the program SPARKY [38].

Supplemental Data

Supplemental Data are available with this article online at http://www.chembiol.com/cgi/content/full/12/10/1137/DC1/.

Acknowledgments

The work was supported by the Bundesministerium für Bildung und Forschung, by the Deutsche Forschungsgemeinschaft (DFG) grants to A.B. and by the Fonds der Chemischen Industrie grant to S.G. The NMR spectrometers are part of the Bavarian NMR Center in Garching. We thank A. Schandelmaier for assistance.

Received: June 6, 2005
Revised: August 1, 2005
Accepted: August 8, 2005
Published: October 21, 2005

References

1. Buzzetti, F., Eisenberg, F., Grant, H.N., Keller-Schierlein, W., Voser, W., and Zähner, H. (1968). Avilamycin. Experientia *24*, 320–324.

2. Weitnauer, G., Hauser, G., Hofmann, C., Linder, U., Boll, R., Pelz, K., Glaser, S.J., and Bechthold, A. (2004). Novel avilamycin derivatives with improved polarity generated by targeted gene disruption. Chem. Biol. *11*, 1403–1411.
3. Belanger, A.E., and Shryock, T.R. (2005). Avilamycin did not play a role in the discontinuation of evernimicin as a clinical drug candidate. J. Mass. Spectrom. *40*, 1109.
4. Belova, L., Tenson, T., Xiong, L., McNicholas, P.M., and Mankin, A.S. (2001). A novel site of antibiotic action in the ribosome: interaction of evernimicin with the large ribosomal subunit. Proc. Natl. Acad. Sci. U. S. A. *98*, 3726–3731.
5. McNicholas, P.M., Najarian, D.J., Mann, P.A., Hesk, D., Hare, R.S., Shaw, K.J., and Black, T.A. (2000). Evernimicin binds exclusively to the 50S ribosomal subunit and inhibits translation in cell-free systems derived from both Gram-positive and Gram-negative bacteria. Antimicrob. Agents Chemother. *44*, 1121–1126.
6. McNicholas, P.M., Mann, P.A., Najarian, D.J., Miesel, L., Hare, R.S., and Black, T.A. (2001). Effects of mutations in ribosomal protein L16 on susceptibility and accumulation of evernimicin. Antimicrob. Agents Chemother. *45*, 79–83.
7. Weitnauer, G., Mühlenweg, A., Trefzer, A., Hoffmeister, D., Sussmuth, R.D., Jung, G., Welzel, K., Vente, A., Girreser, U., and Bechthold, A. (2001). Biosynthesis of the orthosomycin antibiotic avilamycin A: deductions from the molecular analysis of the *avi* biosynthetic gene cluster of *Streptomyces viridochromogenes* Tü57 and production of new antibiotics. Chem. Biol. *8*, 569–581.
8. Treede, I., Hauser, G., Mühlenweg, A., Hofmann, C., Schmidt, M., Weitnauer, G., Glaser, S.J., and Bechthold, A. (2005). Genes involved in the formation and attachment of a two-carbon chain as component of methyleurekanate, a branched chain sugar moiety of avilamycin A. Appl. Environ. Microbiol. *71*, 400–406.
9. Frey, P.A. (1996). The Leloir pathway: a mechanistic imperative for three enzymes to change stereochemical configuration of a single carbon in galactose. FASEB J. *10*, 461–470.
10. Hegeman, A.D., Gross, J.W., and Frey, P.A. (2001). Probing catalysis by *Escherichia coli* dTDP-Glucose-4,6-dehydratase: identification and preliminary characterization of functional amino acid residues at the active site. Biochemistry *40*, 6598–6610.
11. Gebb, C., Baron, D., and Grisebach, H. (1975). Spectroscopic evidence for the formation of a 4-keto intermediate in the UDP-apiose/UDP-xylose synthase reaction. Eur. J. Biochem. *54*, 493–498.
12. Schutzbach, J.S., and Feingold, D.S. (1970). Biosynthesis of uridine diphosphate D-xylose. IV. Mechanism of action of uridine diphosphoglucuronate carboxy-lyase. J. Biol. Chem. *245*, 2476–2482.
13. Jörnvall, H., Persson, B., Krook, M., Atrian, S., Gonzalez-Duarte, R., Jeffery, J., and Ghosh, D. (1995). Short-chain dehydrogenases/reductases (SDR). Biochemistry *34*, 6003–6013.
14. Jörnvall, H. (1999). Multiplicity and complexity of SDR and MDR enzymes. Adv. Exp. Med. Biol. *463*, 359–364.
15. Tanaka, N., Nonaka, T., Nakamura, K., and Hara, A. (2001). SDR structure, mechanism of action, and substrate recognition. Curr. Org. Chem. *5*, 89–111.
16. Beis, K., Allard, S.T.M., Hegeman, A.D., Murshudov, G., Philp, D., and Naismith, J.H. (2003). The structure of NADH in the enzyme dTDP-D-glucose dehydratase (RmlB). J. Am. Chem. Soc. *125*, 11872–11878.
17. Gatzeva-Topalova, P.Z., May, A.P., and Sousa, M.C. (2004). Crystal structure of *Escherichia coli* ArnA (PmrI) decarboxylase domain. A key enzyme for lipid A modification with 4-amino-4-deoxy-L-arabinose and polymyxin resistance. Biochemistry *43*, 13370–13379.
18. Allard, S.T.M., Giraud, M.F., Whitfield, C., Graninger, M., Messner, P., and Naismith, J.H. (2001). The crystal structure of dTDP-D-glucose 4,6-dehydrogenase (RmlB) from *Salmonella enterica* serovar typhimurium, the second enzyme in the dTDP-L-rhamnose pathway. J. Mol. Biol. *307*, 283–295.
19. Bar-Peled, M., Griffith, C.L., and Doering, T.L. (2001). Functional cloning and characterization of a UDP-glucuronic acid decarboxylase: the pathogenic fungus *Cryptococcus neoformans* elucidates UDP-xylose synthesis. Proc. Natl. Acad. Sci. USA *98*, 12003–12008.
20. Kobayashi, M., Nakagawa, H., Suda, I., Miyagawa, I., and Matoh, T. (2002). Purification and cDNA cloning of UDP-D-glucuronate carboxy-lyase (UDP-D-xylose synthase) from pea seedings. Plant Cell Physiol. *43*, 1259–1265.
21. Bililign, T., Shepard, E.M., Ahlert, J., and Thorson, J.S. (2002). On the origin of deoxypentoses: evidence to support a glucose progenitor in the biosynthesis of calicheamicin. Chembiochem *3*, 1143–1146.
22. Flett, F., Mersinias, V., and Smith, C.P. (1997). High efficiency intergeneric conjugal transfer of plasmid DNA from *Escherichia coli* to methyl DNA-restricting streptomycetes. FEMS Microbiol. Lett. *155*, 223–229.
23. MacNeil, D.J., Gewain, K.M., Ruby, C.L., Dezeny, G., Gibbons, P.H., and MacNeil, T. (1992). Analysis of *Streptomyces avermitilis* genes required for avermectin biosynthesis utilizing a novel integration vector. Gene *111*, 61–68.
24. Pelzer, S., Reichert, W., Huppert, M., Heckmann, D., and Wohlleben, W. (1997). Cloning and analysis of a peptide synthetase gene of the balhimycin producer *Amycolatopsis mediterranei* DSM5908 and development of a gene disruption/replacement system. J. Biotechnol. *56*, 115–128.
25. Biermann, M., Logan, R., O'Brien, K., Seno, E.T., Nagaraja, R., and Schoner, B.E. (1992). Plasmid cloning vectors for conjugal transfer of DNA from *Escherichia coli* to *Streptomyces* spp. Gene *166*, 43–49.
26. Hoffmeister, D., Ichinose, K., and Bechthold, A. (2001). Two sequence elements of glycosyltransferases involved in urdamycin biosynthesis are responsible for substrate specificity and enzymatic activity. Chem. Biol. *8*, 557–567.
27. Sambrook, J., Fritsch, E.F., and Maniatis, F. (1989). Molecular Cloning: A Laboratory Manual, Second Edition (Cold Spring Harbor, NY: Cold Spring Harbor Laboratory Press).
28. Hopwood, D.A., Bibb, M.J., Chater, K.F., Kieser, T., Bruton, C.J., Kieser, H.M., Bruton, C.J., Kieser, H.M., Lydiate, D.J., Smith, C.P., et al. (1985). Genetic Manipulation of *Streptomyces*: A Laboratory Manual (Norwich, UK: The John Innes Foundation).
29. Altschul, S.F., Madden, T.L., Schaffer, A.A., Zhang, J., Zhang, Z., Miller, W., and Lipmann, D.J. (1997). Gapped BLAST and PSI-BLAST: a new generation of protein database search programs. Nucleic Acids Res. *25*, 3389–3402.
30. Rance, M., Sorensen, O.W., Bodenhausen, G., Wagner, G., Ernst, R.R., and Wüthrich, K. (1983). Improved spectral resolution in cosy ^{1}H NMR spectra of proteins via double quantum filtering. Biochem. Biophys. Res. Commun. *117*, 479–485.
31. Braunschweiler, L., and Ernst, R.R. (1983). Coherence transfer by isotropic mixing: application to proton correlation spectroscopy. J. Magn. Reson. *53*, 521–528.
32. Bax, A., and Davis, D.G. (1985). Mlev-17-based two-dimensional homonuclear magnetization transfer spectroscopy. J. Magn. Reson. *65*, 355–360.
33. Glaser, S.J., and Quant, J.J. (1996). Homonuclear and heteronuclear Hartmann-Hahn transfer in isotropic liquids. Adv. Magn. Opt. Reson. *19*, 59–252.
34. Bothner-By, A.A., Stephens, R.L., Lee, J.-M., Warren, C.D., and Jeanloz, R.W. (1984). Structure determination of a tetrasaccharide: transient nuclear Overhauser effects in the rotating frame. J. Am. Chem. Soc. *106*, 811–813.
35. Bodenhausen, G., and Ruben, D.J. (1980). Natural abundance N-15 NMR by enhanced heteronuclear spectroscopy. Chem. Phys. Lett. *69*, 185–189.
36. Summers, M.F., Marzilli, L.G., and Bax, A. (1986). Complete H-1 and C-13 assignments of coenzyme-B12 through the use of new two-dimensional NMR experiments. J. Am. Chem. Soc. *108*, 4285–4294.
37. Norwood, T.J., Boyd, J., Heritage, J.E., Soffe, N., and Campbell, I.D. (1990). Comparison of techniques for H-1-detected heteronuclear H-1-N-15 spectroscopy. J. Magn. Reson. *87*, 488–501.
38. Goddard, T.D., and Kneller, D.G. (2001). Sparky 3 (computer program). University of California, San Francisco.